International Journal of Bifurcation and Chaos, Vol. 24, No. 9 (2014) 1450114 (20 pages)

DOI: 10.1142/S0218127414501144

Discrete Switching Host-Parasitoid Models with Integrated Pest Control

Changcheng Xiang* and Zhongyi Xiang†
Key Laboratory of Biologic Resources Protection and Utilization, Hubei Minzu University, Enshi, Hubei 445000, P. R. China
**xcc7426681@126.com*
†*zhyxiang260@yahoo.com.cn*

Sanyi Tang
College of Mathematics and Information Science, Shaanxi Normal University, Xi'an 710062, P. R. China
sytang@snnu.edu.cn

Jianhong Wu
Laboratory for Industrial and Applied Mathematics (LIAM), Department of Mathematics and Statistics, York University, Toronto, M3J 1P3, Canada
wujh@mathstat.yorku.ca

Received January 6, 2014; Revised April 12, 2014

The switched discrete host-parasitoid model concerning integrated pest management (IPM) has been proposed in the present work, and the economic threshold (ET) is chosen to guide the switches. That is, if the density of host (pest) population increases and exceeds the ET, then the biological and chemical tactics are applied together. Those multiple control measures are suspended once the density of host falls below the ET. Firstly, the existence and stability of several types of equilibria of switched system have been discussed briefly, and two- or three-parameter bifurcation diagrams reveal the regions of different types of equilibria including regular and virtual equilibria. Secondly, numerical bifurcation analyses show that the switched discrete system may have very complex dynamics including the co-existence of multiple attractors and switched-like behavior among attractors. Finally, we address how the key parameters and initial values of both host and parasitoid populations affect the host outbreaks, switching frequencies or mean switching frequency, and consequently the relative biological implications with respect to pest control are discussed.

Keywords: Switched host-parasitoid model; integrated pest management; host outbreak; multiple attractors; switching frequency.

1. Introduction

Pest control is a very important issue in agriculture, ecology and fisheries since pest outbreak can lead to huge economic losses [Grainge & Ahmed, 1988]. For example, the 2003–2004 desert locust outbreak resulted in significant economic damage to the agriculture in many areas of northern and western Africa [Ceccato *et al.*, 2007]. Chemical control and biological control have been widely used as two main methods for pest control, and

*Author for correspondence

these approaches are usually adopted simultaneously. More complex Integrated Pest Management (IPM) strategies are designed to combine biological, cultural and chemical tactics to prevent pest outbreak by maintaining the density of pests under consideration below an economic injury level (EIL) [Tang *et al.*, 2008]. IPM was introduced in the late 1970s for agricultural crops [Smith *et al.*, 1976], and was later extended and promoted for the control of apple orchards pests in Europe [Blommers, 1994], the fungal leaf disease in Germany [Wolf & Verreet, 2002], and the tropical rice pests [Settle *et al.*, 1996], among other successful stories.

Chemical control is the most important component of an IPM, because the pesticides can quickly kill the pest insects and prevent the insect density from reaching the EIL. However, there are three disadvantages of using the pesticides. First of all, the pesticides damage the land by killing the natural enemies as well, which in turn would lead to the outbreak of pest population. For example, in tropical Asia, Nilaparvata lugens has become a major pest of rice due to the insecticide-induced resurgence [Heinrichs & Mochida, 1984]. Potato beetle (CPB) outbreak is another example [Reed *et al.*, 2001], where spraying pesticides failed to reduce the concentration of target organisms, but led to the increase of the concentration of potato beetle. Chemical pesticides are not always effective due to the pesticide resistance, as shown in the study of long-term residual effects of pesticide using impulsive differential equations model [Liang *et al.*, 2013; Tang *et al.*, 2013]. Finally, long-term use of pesticide can cause significant environment pollution.

Biological control is another key component of an IPM strategy [Parker, 1971; Helyer *et al.*, 2014]. There are three basic types of biological pest control strategies: importation, augmentation and conservation [Van Lenteren & Woets, 1988]. To reduce the pest populations, we should release natural enemies, such as predators, parasitoids, pea aphid, and pathogens [Mound & Halsey, 1978; Mitchell & Power, 2003]. In early pest infestations or small pest population, the periodic inundative releases are necessary to achieve an adequate parasitism level. For instance, the periodic inundative releases of the parasitoid *Encarsia formosa* were successfully used to control greenhouse *whitefly* [Hoffmann & Frodsham, 1993]. Under conditions of high pest incidence, the inoculative release is sufficient to achieve a comparatively high parasitism level, as shown in the use of the *Trichogramma Ostriniae* for controlling the *European Ostrinia Nubilalis* [Wright *et al.*, 2002]. The two release methods were used simultaneously for managing the outbreak of South American tomato *pinworm*, *Tuta absoluta* (*Meyrick*). Another example is the application of the egg-parasitoid *Trichogramma achaeae Nagaraja and Nagarkatti* to control the *pin worm*, using the inundative release early in the growing season and then the inoculative release during the pest outbreak [Cabello *et al.*, 2012].

An important concept in IPM is economic threshold (ET) [Tang *et al.*, 2008; Higley & Pedigo, 1996] that is determined by the social, economic, ecological consideration. We should spray pesticide and release natural enemies only after the economic threshold is reached or exceeded. Liang and Tang [2010] considered several pest control models with ET and taking into account pesticides sprayed at fixed or variable moments in order to find optimal time and dosage of pesticides spraying. This optimal timing of pesticides spraying is also important since no measure needs to be taken for some pests during particular periods, for example, the change of *caterpillars* from an active feeding (larva) to a nonfeeding stage (pupa) during their development often produces a natural decline without any control [Jenser *et al.*, 1999].

The host-parasitoid dynamics with integrated pest control is naturally modeled by the so-called switching systems (or Filippov systems). Such systems based on the ODE model for the host-parasitoid interaction have been studied in recent literature, see [Tang *et al.*, 2012] for relevant references. The simplest switching system depicted by a discrete Ricker equation has also been used for locust control [Holt & Cheke, 1996]. Here, we formulate and analyze a switching discrete model with IPM based on the Nicholson–Bailey model, and subject to the guidance for switching by an economic threshold (ET). In our consideration, biological and chemical tactics are applied together if the density of host (pest) population increases and exceeds the ET, and these measures are suspended once the host density falls below the ET. We discuss the existence and stability of several types of equilibria of the switching system, and conduct a bifurcation analysis to generate bifurcation diagrams for the existence and change of different types of, regular and virtual, equilibria. We also perform some numerical bifurcation analyses to show that the

proposed simple switching discrete system may have very complex dynamics including the coexistence of multiple attractors, and the oscillatory behaviors switching among attractors. We also address the issue of how key control parameters and initial values of both host and parasitoid populations affect the host outbreaks.

2. Switching Host-Parasitoid Model

The well-known discrete single-population Moran–Ricker model [Ricker, 1954; Moran, 1950] is given by

$$H(t+1) = H(t)\exp\left[r\left(1 - \frac{H(t)}{K}\right)\right], \qquad (1)$$

where $H(t)$ denotes the density of the host population in generation t, r represents the intrinsic growth rate, and K is the carrying capacity of the environment. Denoting the parasitoid population size in generation t as $P(t)$ and the probability of a host being encountered by any parasitoid as β, the typical Nicholson–Bailey host-parasitoid model can be expressed in the form

$$\begin{cases} H(t+1) = H(t)\exp\left[r\left(1 - \frac{H(t)}{K}\right) - \beta P(t)\right], \\ P(t+1) = H(t)[1 - \exp(-\beta P(t))], \end{cases} \qquad (2)$$

where the term $\exp[-\beta P(t)]$ is the probability that a host individual escapes from parasitism.

Based on model (2), the following discrete-generation host-parasitoid model was developed [Rohani & Ruxton, 1999; Hassell & May, 1973]

$$\begin{cases} H(t+1) = H(t)\exp\left[r\left(1 - \frac{H(t)}{K}\right) - \beta P(t)\right], \\ P(t+1) = H(t)[1 - \exp(-\beta P(t))] + \sigma P(t), \end{cases} \qquad (3)$$

where σ denotes the survival rate of parasitoid populations from t generation to next generation.

If the host population represents the pests and parasitoid population the natural enemy, then the model describes the pest-natural enemy interaction. To take into account the IPM strategies for controlling the pest population, Tang *et al.* [2008] assumed that at every qth generation the system (3) is subject to a perturbation resulting in a proportional decrease of the insect pest and an introduction of the parasitoid with a population sizes-independent constant τ. This led to the following discrete host-parasitoid model with fixed moments

$$\begin{cases} \left.\begin{aligned} H(t+1) &= H(t)\exp\left[r\left(1 - \frac{H(t)}{K}\right)\right], \\ P(t+1) &= H(t)[1 - \exp(-\beta P(t))] + \sigma P(t), \end{aligned}\right\} \quad t = 0, 1, 2, \ldots; \\ \left.\begin{aligned} H_{qk^+} &= (1 - q_1)H_{qk}, \\ P_{qk^+} &= (1 + q_2)P_{qk} + \tau, \end{aligned}\right\} \quad k = 1, 2, \ldots. \end{cases} \qquad (4)$$

It was shown in [Tang *et al.*, 2008] that this model can exhibit rich dynamic behaviors including host-eradication, host-parasitoid persistence and host-outbreak solutions.

However, in the above model, the impulsive perturbations were implemented for pest and parasitoid populations at fixed generations no matter whether the density of pest population exceeds the ET or not. This is cost ineffective, and in practice, IPM strategies are only implemented when the density of pest population exceeds the ET, and these strategies are suspended once the pest population density falls below the ET.

Therefore, based on the typical Nicholson–Bailey host-parasitoid model (2), only when the density of host population exceeds the threshold level ET, a chemical control tactic is applied with a proportional killing rate p in conjunction with a biological control measure with a constant releasing number τ. This yields naturally the following control model with IPM tactics

$$\left.\begin{cases} H(t+1) = (1-p)H(t) \\ \qquad\qquad \times \exp\left[r\left(1 - \frac{H(t)}{K}\right) - \beta P(t)\right], \\ P(t+1) = H(t)[1 - \exp(-\beta P(t))] + \tau, \end{cases}\right\} \quad \text{when } H(t) \geq ET, \qquad (5)$$

where $0 \leq p < 1$ and $\tau \geq 0$. In particular, if $p = 0$ and $\tau > 0$, then only the biological control measures are applied; and if $p > 0$ and $\tau = 0$, then only the chemical control tactics are applied. In the following, we assume $p\tau \neq 0$ so at least one control measure is applied once the density of pest population exceeds the ET.

Consequently, combining the model with IPM when the density of pest population exceeds the ET and the model without control tactics when the density falls below the ET, we have the following switching system

$$\begin{cases} \left.\begin{aligned} H(t+1) &= H(t)\exp\left[r\left(1-\frac{H(t)}{K}\right)-\beta P(t)\right], \\ P(t+1) &= H(t)[1-\exp(-\beta P(t))], \end{aligned}\right\} & \text{when } H(t) < ET; \\ \left.\begin{aligned} H(t+1) &= (1-p)H(t)\exp\left[r\left(1-\frac{H(t)}{K}\right)-\beta P(t)\right], \\ P(t+1) &= H(t)[1-\exp(-\beta P(t))]+\tau, \end{aligned}\right\} & \text{when } H(t) \geq ET. \end{cases} \tag{6}$$

We should mention that switching systems (or Filippov systems) described by an ODE system have now been widely used in ecosystem management with a threshold control policy [Bischi *et al.*, 2013; Bischi *et al.*, 2014; Tang *et al.*, 2012]. Switching systems based on difference equations have also been used for locust control [Holt & Cheke, 1996], where the discrete switching Moran–Ricker model was used and the intrinsic growth rate and carrying capacity of locust population are assumed different during different growth phases. In our present study, we focus on the switching model (6) and explore its complex dynamical behaviors using some bifurcation analysis. We aim to use the switching frequencies between two subsystems as key bifurcation parameters, and linking the bifurcation values to key control parameters such as the killing rate p, the releasing constant τ and the threshold value ET.

3. Equilibrium of Two Subsystems and Their Stability

For convenience, we denote $F(H(t)) = H(t) - ET$ and $Z(t) = [H(t), P(t)]^T$, so system (6) can be rewritten as

$$\begin{aligned} S_{G_1}(t+1) &= [H(t)e^{r(1-\frac{H(t)}{K})-\beta P(t)}, \\ &\quad H(t)(1-e^{-\beta P(t)})]^T, \\ S_{G_2}(t+1) &= [(1-p)H(t)e^{r(1-\frac{H(t)}{K})-\beta P(t)}, \\ &\quad H(t)(1-e^{-\beta P(t)})+\tau]^T, \end{aligned} \tag{7}$$

where the two regions G_1 and G_2 are defined as follows

$$G_1 = \{(H,P)\,|\,F(H) < 0, H > 0, P > 0\},$$
$$G_2 = \{(H,P)\,|\,F(H) \geq 0, H > 0, P > 0\}.$$

In the rest of this paper, we call the system (7) defined in region G_1 as subsystem S_{G1}, and in region G_2 as subsystem S_{G2}. Although the existence and stability of equilibria of subsystem S_{G_1} have been investigated by [Hassell & May, 1973], we first address this for both subsystems briefly, which are useful for discussing the types of the equilibria of whole switching system (7).

3.1. *Equilibria of the subsystems S_{G1} and S_{G2}*

For subsystem S_{G1}, let $H_t = H_{t+1} = H_{1*}$ and $P_t = P_{t+1} = P_{1*}$. Then the equilibrium (H_{1*}, P_{1*}) satisfies the following equations

$$H_* = H_*\exp\left(r\left(1-\frac{H_*}{k}\right)-\beta P_*\right),$$
$$P_* = H_*(1-\exp(-\beta P_*)).$$

Obviously, there exists an extinction steady state $E_{00} = (0,0)$, and a boundary steady state $E_{+0} = (K,0)$. For the existence of an interior steady state $E_{1*} = (H_{1*}, P_{1*})$, we consider the following equations

$$\begin{cases} r\left(1-\frac{H_{1*}}{K}\right)-\beta P_{1*} = 0, \\ P_{1*} = H_{1*}(1-\exp(-\beta P_{1*})). \end{cases} \tag{8}$$

Solving H_{1*} from the first equation of (8) and submitting it into the second equation, one yields

$$\frac{P_*}{K} = \left(1-\frac{\beta P_*}{r}\right)(1-e^{-\beta P_*}). \tag{9}$$

Define two auxiliary functions:

$$\begin{cases} f(x) = \dfrac{x}{K}, \\ g(x) = \left(1 - \dfrac{\beta x}{r}\right)(1 - e^{-\beta x}). \end{cases} \tag{10}$$

It is clear that $f(0) = g(0) = g(r/\beta) = 0$, which indicates that both functions f and g intersect at the unique point $x_* > 0$ provided that $f'(0) < g'(0)$. Therefore, when $\frac{1}{K} < \beta$, there exists a unique $P_{1*} > 0$ such that $f(P_{1*}) = g(P_{1*})$.

Similarly, we can discuss the existence of equilibria of subsystem S_{G2}. Note that S_{G2} has a boundary steady state $E'_{+0} = (0, \tau)$ if $\tau > 0$, and the interior steady state $E_{2*} = (H_{2*}, P_{2*})$ satisfies the following equation

$$\frac{P_{2*}}{K} - \left(1 - \frac{\beta P_{2*} - \ln(1-p)}{r}\right)(1 - e^{-\beta P_{2*}}) = \tau. \tag{11}$$

Define the following three auxiliary functions

$$\begin{cases} h(x) = \dfrac{x}{K} - \tau, \\ h_1(x) = \dfrac{x}{K}, \\ q(x) = \left(1 - \dfrac{\beta x - \ln(1-p)}{r}\right)(1 - e^{-\beta x}). \end{cases} \tag{12}$$

It is easy to show that $h(0) + \tau = h_1(0) = q(0) = q((r + \ln(1-p))/\beta) = 0$. Based on the above discussions, we know that the two functions $h_1(x)$ and $q(x)$ intersect at a unique point $x_* > 0$ provided that $0 < h'_1(0) < q'(0)$. This implies that when $\frac{1}{K} < \frac{\ln(1-p)\beta}{r}$ there exists $P_* > 0$ such that $h_1(P_*) = q(P_*)$. Since $h(x) = h_1(x) - \tau$ and $h'(0) = h'_1(0) < q'(0)$, both functions $h(x)$ and $q(x)$ intersect provided that $0 < K\tau \le (r + \ln(1-p))/\beta$. Therefore, there exists a $P_{2*} > 0$ such that $h(P_{2*}) = q(P_{2*})$ if

$$\frac{r}{\ln(1-p)\beta} < K \le \frac{(r + \ln(1-p))}{\beta\tau}. \tag{13}$$

In order to show the existence of an interior equilibrium of subsystem S_{G_2}, we plot all three functions with different values of τ, as indicated in Fig. 1.

3.2. *Stability of equilibria of subsystems S_{G1} and S_{G2}*

The local stability of $E_{1*} = (H_{1*}, P_{1*})$ of subsystem S_{G_1} is determined by the eigenvalues of following Jacobian matrix

$$J_1 = \begin{pmatrix} 1 - r + \beta P_{1*} & -\beta H_{1*} \\ \dfrac{P_{1*}}{H_{1*}} & \beta(H_{1*} - P_{1*}) \end{pmatrix}. \tag{14}$$

It follows from the equation (9) that we have

$$J_1 = \begin{pmatrix} \dfrac{K - rH_{1*}}{K} & -\beta H_{1*} \\ \dfrac{r(K - H_{1*})}{\beta K H_{1*}} & \dfrac{\beta K H_{1*} - rK + rH_{1*})}{K} \end{pmatrix}. \tag{15}$$

Its characteristic equation is

$$P(\lambda) = \lambda^2 - \mathrm{Trace}(J)\lambda + \mathrm{Det}(J), \tag{16}$$

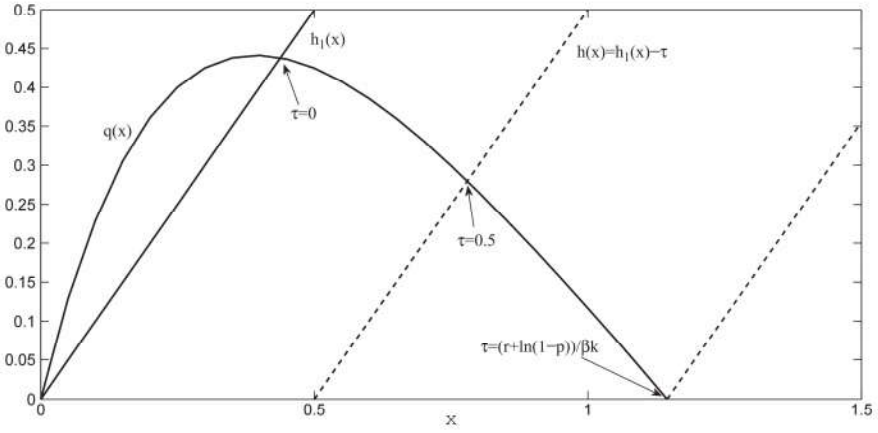

Fig. 1. Existence of the equilibrium $E_{2*} = (H_{2*}, P_{2*})$ of subsystem S_{G2}. The parameters are fixed as $\beta = 3$; $k = 1$, $r = 3.5$, $p = 0.1$.

where $\text{Trace}(J) = 1 - r + \beta H_{1*}$, $\text{Det}(J) = \frac{-(rK\beta+r^2)}{K^2}H_{1*}^2 + \frac{(K\beta+r^2)}{K}H_{1*}$. According to the Jury criteria [Murray, 2002; Elaydi, 2005] the local stability conditions of equilibrium E_{1*} are $|\text{Trace}(J)| < 1+\text{Det}(J) < 2$. That is, if the following inequalities

$$\begin{cases} (rK\beta + r^2)H_{1*}^2 < Kr^2H_{1*} + rK^2, \\ (rK\beta + r^2)H_{1*}^2 > (2-r)K^2 \\ \qquad\qquad + K(2K\beta + r^2)H_{1*}, \\ (rK\beta + r^2)H_{1*}^2 > -K^2 + K(K\beta + r^2)H_{1*} \end{cases} \tag{17}$$

hold true, then E_{1*} is locally asymptotically stable.

Similarly conditions can be obtained for the interior equilibrium E_{2*} of subsystem S_{G_2}.

3.3. *Equilibria for the switching system (7)*

Filippov systems or switching systems have different types of equilibria, and these play a key role in the dynamical behaviors. The classification and stability of these equilibria have been discussed in disease and pest control, for example, Xiao *et al.* [2012] analyzed the emerging infectious disease outbreak control, Xiao *et al.* [2013] discussed the drug response treatment for HIV infected patients, and Tang *et al.* [2012] demonstrated pest control with economic threshold. We now define regular equilibria and virtual equilibria for discrete switching systems.

Definition 3.1. A point $Z_* = (H_*, P_*)$ is called a regular equilibrium of system (7) if Z_* is an equilibrium of subsystem S_{G_1} and $F(H_*) < 0$; or if Z_* is an equilibrium of subsystem S_{G_2} and $F(H_*) \geq 0$. These equilibria will be denoted by $E^r_{S_{G_1}}$ and $E^r_{S_{G_2}}$, respectively. A point Z_* is called a virtual equilibrium of system (7) if Z_* is an equilibrium of subsystem S_{G_1} and $F(H_*) \geq 0$; or if Z_* is an equilibrium of subsystem S_{G_2} and $F(H_*) < 0$. These equilibria will be denoted by $E^v_{S_{G_1}}$ and $E^v_{S_{G_2}}$, respectively.

It is difficult to find closed forms for the interior equilibria of two subsystems, we will employ numerical methods to examine the existence of different types of equilibria and show their coexistence. Therefore, in the following, we first choose r and ET as bifurcation parameters and fix all others as given in Fig. 2(a).

Letting ET vary from 0.1 to 1, r vary from 0.1 to 4 and $\beta = 3$ in Fig. 2(a), we observe that the parameter space is divided into six regions. Note that these parameter regions, and hence the existences of equilibria, depend on the value of r and ET. For example, when the intrinsic growth rate r is relatively small (here $r \in [0.1, 0.5]$), there

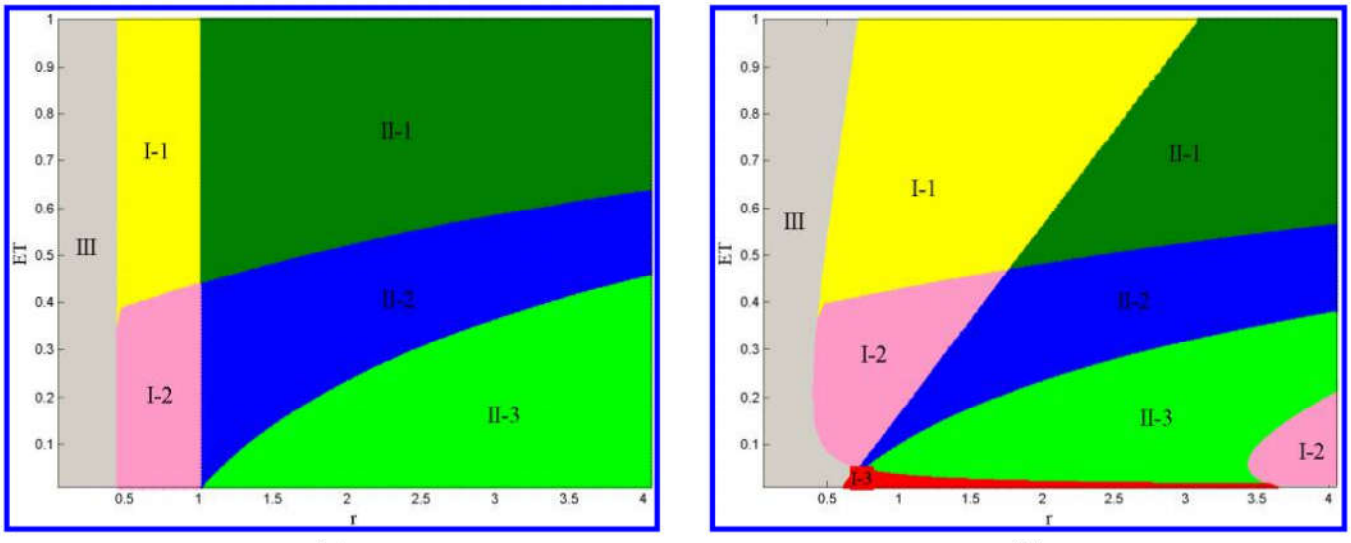

(a) (b)

Fig. 2. Parameter bifurcation diagram for the existence of equilibria of system (7). Here the others are fixed as follows: $p = 0.1, k = 1, \tau = 0.5$. (a) Two-parameter bifurcation diagram of which r and ET are selected as bifurcation parameters, where $r \in [0.1, 4]$, $ET \in [0.01, 1]$ and $\beta = 3$ and (b) three-parameter bifurcation diagram in r–ET plane, where $r \in [0.1, 4]$, $ET \in [0.1, 1]$ and $\beta \in [1, 4]$, simultaneously.

does not exist any interior equilibria, as indicated in region III. If the intrinsic growth rate r lies in $[0.5, 1]$, then there are two regions indicated in I-1 and I-2: in region I-1 only $E^v_{S_{G_1}}$ exists, while in region I-2 only $E^v_{S_{G_2}}$ exists. Moreover, if we let $r = 0.6$, it follows from region I-2 of Fig. 2(a) with $ET = 0.3$. In this case, the unique interior equilibrium of system S_{G_2} is virtual (here $E^v_{S_{G_2}}$), there is no interior equilibrium of system S_{G_1}. As ET increases and exceeds a certain threshold value (here $ET = 0.38$, as shown in region I-1), the virtual equilibrium $E^v_{S_{G_2}}$ disappears, and only the virtual equilibrium $E^v_{S_{G_1}}$ appears in the region I-1. If the intrinsic growth rate r is relatively large (here $r \in [1, 4]$), then there are three regions as indicated as II-1, II-2 and II-3. We observe that in region II-1, $E^r_{S_{G_1}}$ and $E^v_{S_{G_2}}$ coexist; in region II-2, $E^v_{S_{G_1}}$ and $E^v_{S_{G_2}}$ coexist; in region II-3, $E^v_{S_{G_1}}$ and $E^r_{S_{G_2}}$ coexist. For example, we let $r = 2$ and $ET = 0.15$ from region II-3, the unique interior equilibrium of system S_{G_1} is virtual (here $E^v_{S_{G_1}}$), while the unique interior equilibrium of system S_{G_2} is regular (here $E^r_{S_{G_2}}$). When ET increases and exceeds a certain threshold value (here $ET = 0.2$), the regular equilibrium $E^r_{S_{G_2}}$ becomes a virtual equilibrium $E^v_{S_{G_2}}$, the virtual equilibrium $E^v_{S_{G_1}}$ remains virtual, as shown in region II-2. As ET further increases and exceeds another threshold value (here $ET = 0.46$), the virtual equilibrium $E^v_{S_{G_1}}$ becomes a regular equilibrium $E^r_{S_{G_1}}$ and the virtual equilibrium $E^v_{S_{G_2}}$ remains virtual.

To show the effects of other parameters on the parameter regions, we carry out three-parameter bifurcation analyses, i.e. we also let parameter β vary from 1 to 4 and plot the r–ET plane, as shown in Fig. 2(b). From this plot, we can see that the shapes of all regions are changed. Moreover, a new region I-3 is generated in which equilibrium $E^v_{S_{G_2}}$ occurs, and region I-2 is split into two subregions.

It is clear that if one or more parameters changes, a number of bifurcations occur in Figs. 2(a) and 2(b). One of the main purposes here is to design optimal control strategies to prevent pest outbreaks or keep the density of pest population below ET. From the mathematical point of view, this can be realized if the system can stabilize at the desired level through the integration of different control strategies. To realize this purpose, we can choose the desirable threshold level (here ET) such that all equilibria of each system such as system S_{G_1} and system S_{G_2} become virtual. This control strategy is important for pest control [Tang *et al.*, 2012; Zhao & Xiao, 2013], has been used for fisheries resources management [da Silveira Costa & Meza, 2006; Dercole *et al.*, 2007]. For example, we could choose the corresponding threshold level (ET) such that the interior equilibrium of S_{G_1} becomes virtual, and the interior equilibrium of S_{G_2} becomes virtual. In Fig. 2, the parameter space which lies in the region II-2 meets this kind of objective. For regions II-1 and II-3, we should select the suitable parameters r and ET, change the regular equilibrium of S_{G_1} or S_{G_2} system to be virtual (see Fig. 2). Thus, from the perspective of pest management, the appropriate control strategies and ET should be designed such that the interior equilibrium of S_{G_1} and S_{G_2} are virtual simultaneously.

4. Numerical Analysis of System (7) with *ET*

In this section, we provide the numerical investigations of system (7). In particular, we carry out the bifurcation analysis which can reveal the existence of multiple attractors, coexistence, initial sensitivity and switching behaviors.

4.1. *Bifurcation analysis and chaos*

In order to gain preliminary insights into the properties of the dynamical system, we first give the one-dimensional bifurcation diagrams on the parameter of intrinsic growth rate r and killing rate p. The analyses are expected to reveal the types of attractors, and their changes with parameter variations.

We first choose r as the bifurcation parameter and fix all other parameters as follows: $p = 0.2, ET = 0.51, \beta = 3.98, \tau = 0.1$ and initial values $(H_0, P_0) = (0.2, 0.5)$. It follows from Fig. 3 that the switching host-parasitoid system can exhibit very complex dynamics as the intrinsic growth rate increases. Especially, the host and parasitoid can coexist for a large range of r. When r is increased from 2.5 to 3.2, we can find periodic, quasi-periodic, chaotic solutions, Hopf or period-doubling bifurcations. As the parameter r further increases from 2.6 to 2.84, the system's behaviors suddenly change to chaotic. Moreover, the quasi-periodic attractor abruptly appears at $r = 2.93$, at which the quasi-periodic attractor in the phase plane gives four closed curve [see Fig. 4(b)].

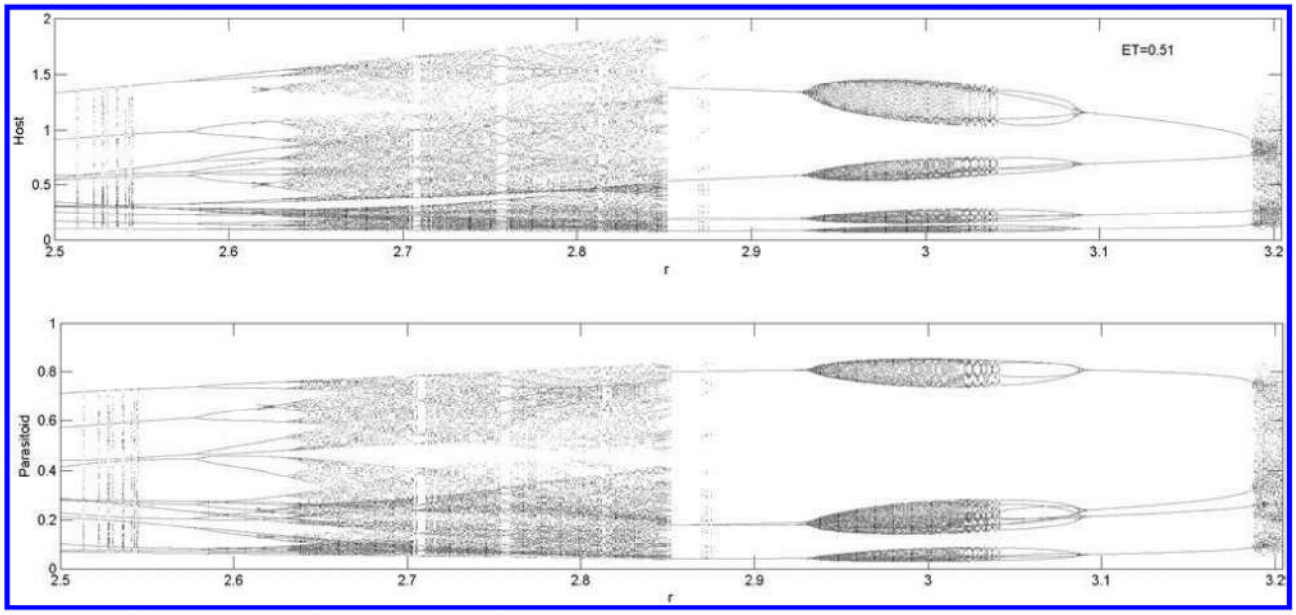

Fig. 3. Bifurcation diagrams of model (4). For each r, the first 1101 simulated values are omitted to remove the initial transients and only the next 100 values are plotted. The host and parasitoid populations are plotted for 500 values of r over [2.5, 3.2]. The other parameters are fixed as $p = 0.2$, $ET = 0.51$, $\beta = 3.98$, $\tau = 0.1$, and the initial value $(H_0, P_0) = (0.2, 0.5)$.

The quasi-periodic attractor disappears and goes to a period solution with period-16 at $r = 3.05$. Once the bifurcation parameter r exceeds the threshold value around 3.09, then a period-halving bifurcation occurs. Furthermore, a chaotic attractor emerges abruptly at $r = 3.19$ [see Fig. 4(a)]. Meanwhile, we can also find from the bifurcation diagram that the model (7) exists with multiple attractors for a range of parameter values, for example $r \in [2.5, 2.55]$ and $[2.85, 2.89]$. We will address this in more detail in the coming subsections.

It follows from the bifurcation diagram of parameter p that the host population can outbreak for small and large killing rates of pesticides, as shown in Fig. 5. Most importantly, Fig. 5 clearly shows how to choose suitable killing rate such that

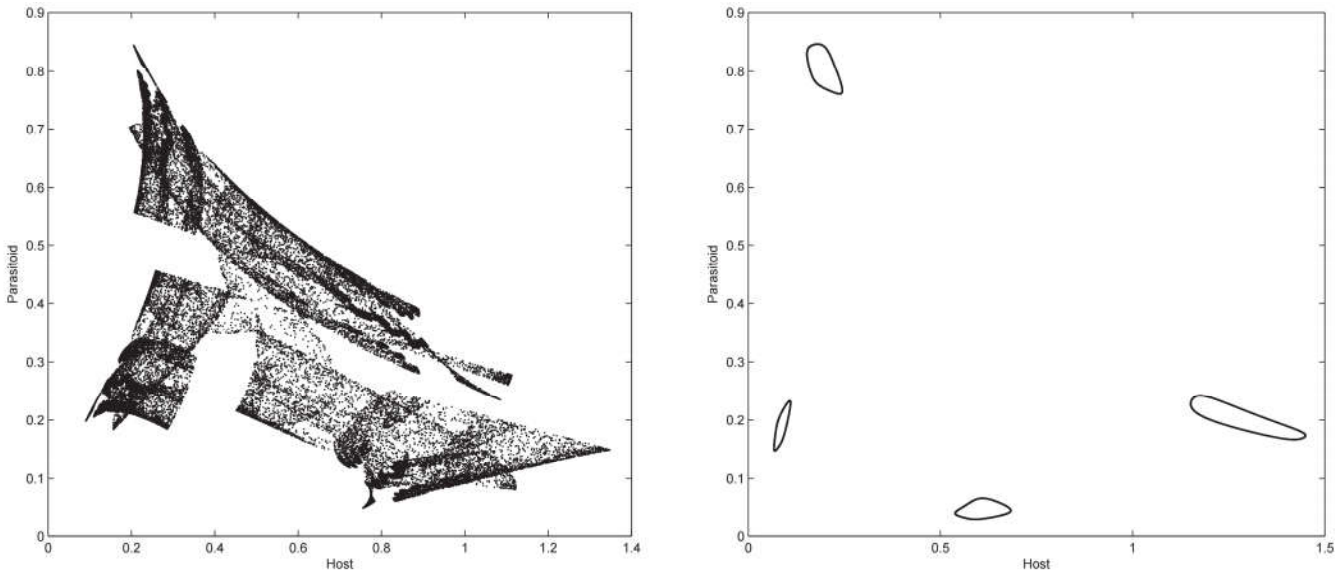

Fig. 4. Phase diagram of model (4), the parameters are fixed as $p = 0.2$, $ET = 0.51$, $\beta = 3.98$, $\tau = 0.1$, and the initial value $(H_0, P_0) = (0.2, 0.5)$. (a) Strange attractor with $r = 3.2$ and (b) quasi-periodic solution with $r = 2.95$.

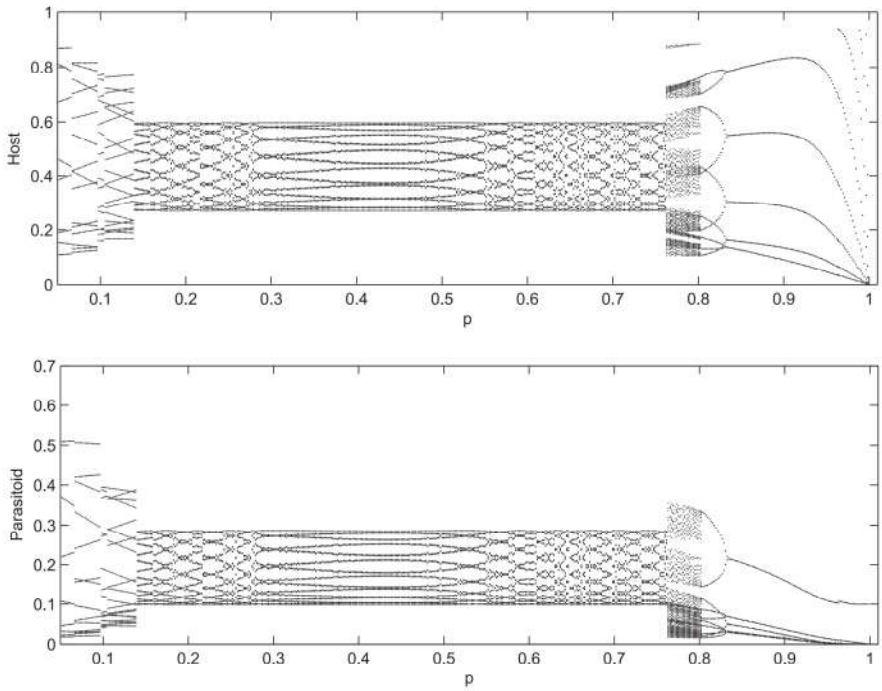

Fig. 5. Bifurcation diagrams of model (4). For each p, the first 1101 simulated values are omitted to remove the initial transients and only the next 100 values are plotted. The host and parasitoid populations are plotted for 500 values of p over [0.01, 1]. The other parameters are fixed as $r = 1$, $ET = 0.7$, $\beta = 3.2$, $\tau = 0.1$, and the initial value $(H_0, P_0) = (0.9, 3.5)$.

the whole system can stabilize at the subsystem S_{G_1} and provide a possible explanation on the Volterra principle. In particular, if $p \in [0.01, 0.12]$, i.e. small killing rate is chosen, then the host population can outbreak (here and in what follows, outbreak means that the density of host population is larger than ET); If $p \in [0.77, 0.95]$, i.e. large killing rate is chosen, then we can see that the host population can still outbreak. This is because the natural enemies may be drastically affected due to less of food. However, if we carefully choose the killing rate (for example, $p \in [0.13, 0.76]$), then the host population can stabilize in the subsystem S_{G_1}. All of these confirm that the interaction between host and parasitoid plays a very important role in pest control, and the control tactics should be designed by considering this interaction.

4.2. *Initial sensitivities, multiple attractors and coexistence*

It is well known that different initial densities of both host and parasitoid populations can result in different dynamics, in particular, different outbreak patterns. Moreover, coexistence of multiple attractors also depends on the initial densities of the host and parasitoid populations. Therefore, we will focus on how the initial densities affect the final states or host outbreaks, and consequently successful pest control.

4.2.1. *Initial sensitivities*

It follows from the bifurcation diagrams (i.e. Fig. 5) that the host population can stabilize in the subsystem S_{G_1}. One interesting question is that, for a given ET, how do the initial densities of host and parasitoid populations affect the control strategies. In particular, what we want to know is how the ET and various pest-natural enemy initial regions affect the controls strategies. To show this, we fix all parameter values as those in Fig. 6. The results shown in Fig. 6 provide some examples of different possible cases. In Fig. 6(a) the initial densities of pest-natural enemy populations are $(0.5, 0.3)$ and the simulation result indicates that the density of the pest population never reaches the given ET (here $ET = 0.7$), which shows that the solution initiating from $(0.5, 0.3)$ is free from IPM tactics. If we set the initial densities as $(0.5, 0.3)$, Fig. 6(b) indicates that the system is free from IPM measures eventually after chemical and biological control tactics are applied several times. If we set the initial densities as $(0.5, 0.45)$ or $(0.4, 0.4)$, the results

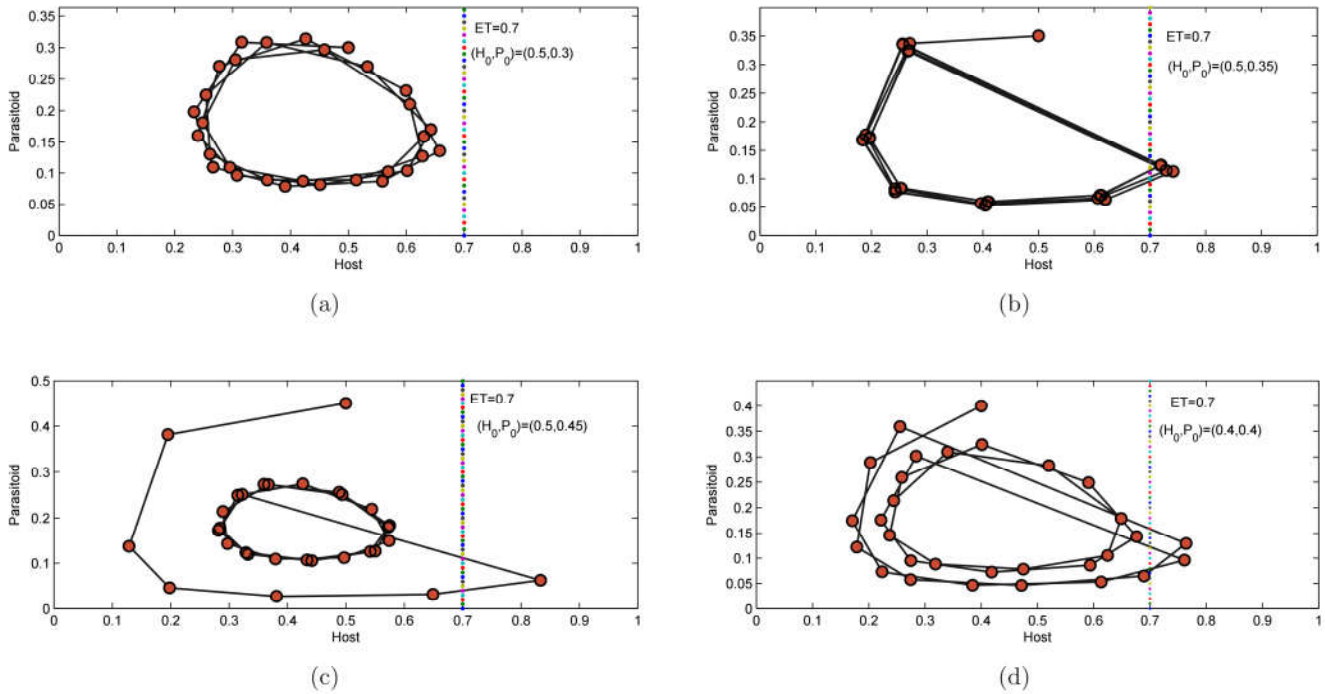

Fig. 6. Illustrating the switch effects of initial densities of the host and parasitoid populations of model (4) on IPM. The parameters are fixed as $r = 1$, $ET = 0.7$, $\beta = 3.2$, $\tau = 0.1$, $k = 1$. The initial densities (H_0, P_0) in (a)–(d) are $(0.5, 0.3)$, $(0.5, 0.35)$, $(0.5, 0.45)$ and $(0.4, 0.4)$, respectively.

indicate that the system is free from IPM control after one or two IPM strategies [see Fig. 6(c) or 6(d)]. Moreover, if we further discuss the above cases on the host densities and the parasitoid densities plane [see Fig. 7(a)], and Fig. 7(b) is an enlargement of Fig. 6(a), which shows that there exist five different regions which are denoted by I, II, III, IV, V with different colors. In region I, the

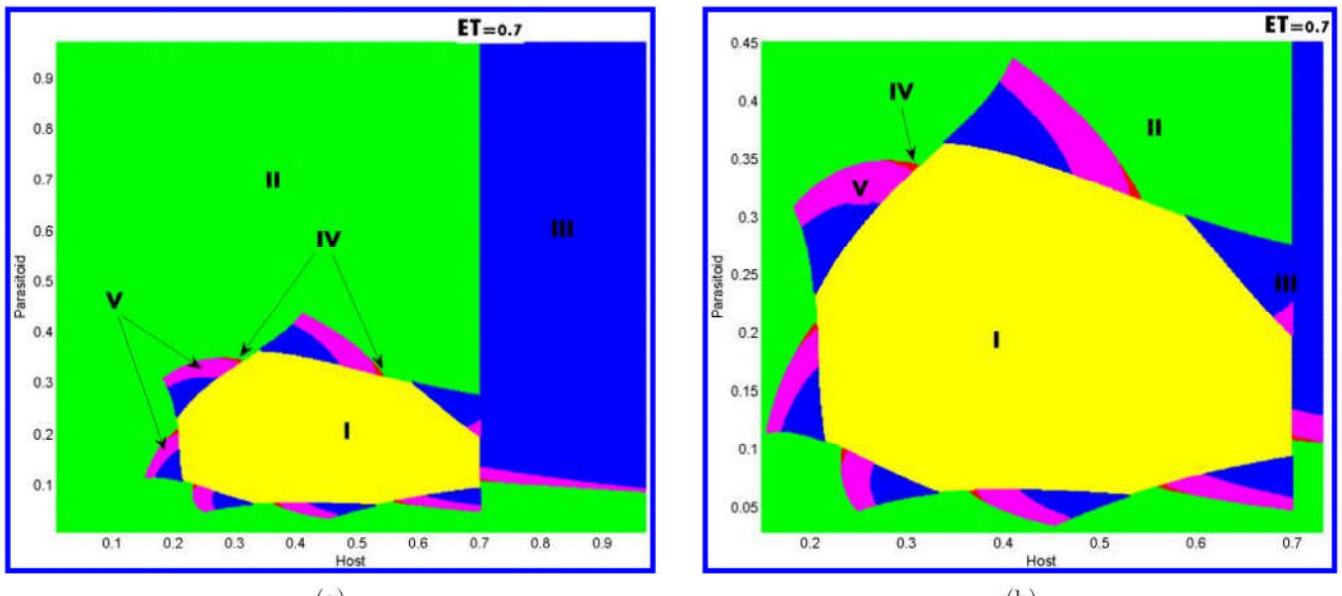

Fig. 7. Illustrating how the pest outbreak frequencies depend on initial densities of the host and parasitoid populations of model (4) on IPM. The parameters are fixed as $p = 0.6$, $r = 1$, $ET = 0.7$, $\beta = 3.2$, $\tau = 0.1$, $k = 1$. The regions I–V denote without pest outbreak, with one, two, three and many times pest outbreak, respectively. (a) The initial densities of the host and parasitoid population both vary from 0 to 1 and (b) the enlargement of (a).

pest population never outbreaks and is always stabilized in the subsystem S_{G_1}, as shown in Fig. 6(a). In region II or III, the system is free from IPM control after one or two IPM applications [for example, Fig. 6(c) or 6(d)]. In region IV, we should apply IPMs three times to let the system be free. In region V, there exist pest outbreaks several times before the system stabilizes in the S_{G_1} subsystem. However, when the initial density of host population is above ET, if we increase the initial densities of the parasitoid population above 0.2, we only spray IPMs two times to let the system be free from control tactics. Therefore, these results confirm that different host-parasitoid initial densities as well as host-parasitoid ratios may result in different final states of the host population.

4.2.2. *Multiple attractors and coexistence*

As mentioned before, the switching host-parasitoid system reveals lots of new dynamic behavior including the coexistence of multiattractors. To confirm this and discuss their biological implications, we fix all parameters as those in Fig. 8 and choose different initial densities. For example, three host-outbreak attractors coexist at $r = 2.54$, as shown in Fig. 8, from which we can see that these host-outbreak attractors display different amplitudes and frequencies. If we let the initial values be $(H_0, P_0) = (0.1, 1.5)$, then the solution of system (4) approaches the first attractor [Figs. 8(a) and 8(b)] which oscillates with period 3. Note that this attractor shows that it will take three host generations for host population outbreak with a middle size. If we choose the initial value $(H_0, P_0) = (2.1, 0.3)$, then the outbreak patterns for host population are quite complex, as shown in Figs. 8(c) and 8(d), from which we can see that the maximal amplitude is relatively large. The third attractor is shown in Figs. 8(e) and 8(f) with a outbreak frequency one, where the initial value is $(H_0, P_0) = (0.1, 1.6)$. By comparing these three attractors, we conclude

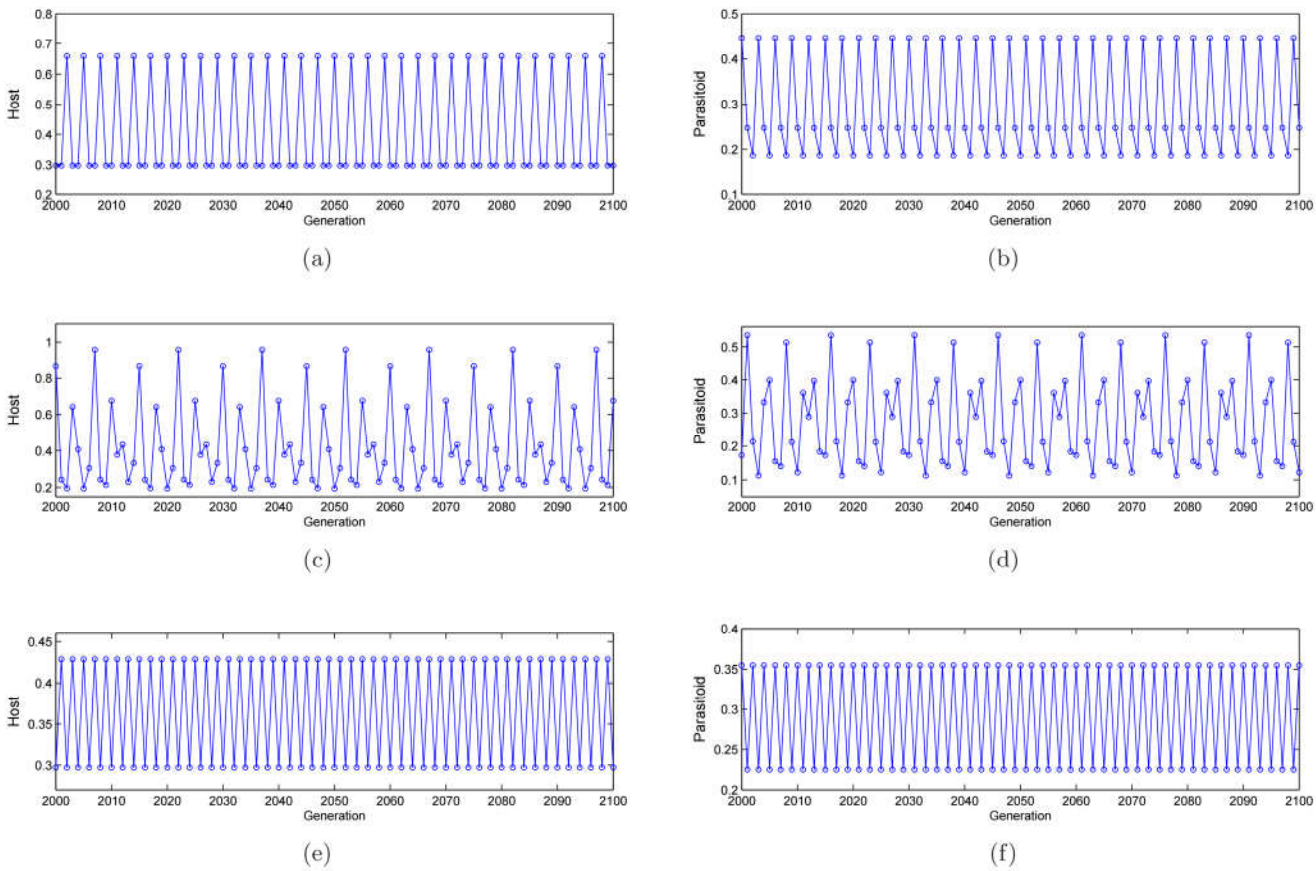

Fig. 8. Three coexisting attractors of system (7) with different initial values. The initial conditions from top to bottom are $(H_0, P_0) = (0.1, 1.5)$, $(2.1, 0.3)$ and $(0.1, 1.6)$ respectively. (a) and (b) Periodic attractor with period 3; (c) and (d) periodic attractor with period 15; (e) and (f) periodic attractor with period 2. The parameters are fixed as follows: $r = 2.54$, $p = 0.6$, $ET = 0.4$, $\beta = 4$, $\tau = 0.1$, $k = 1$.

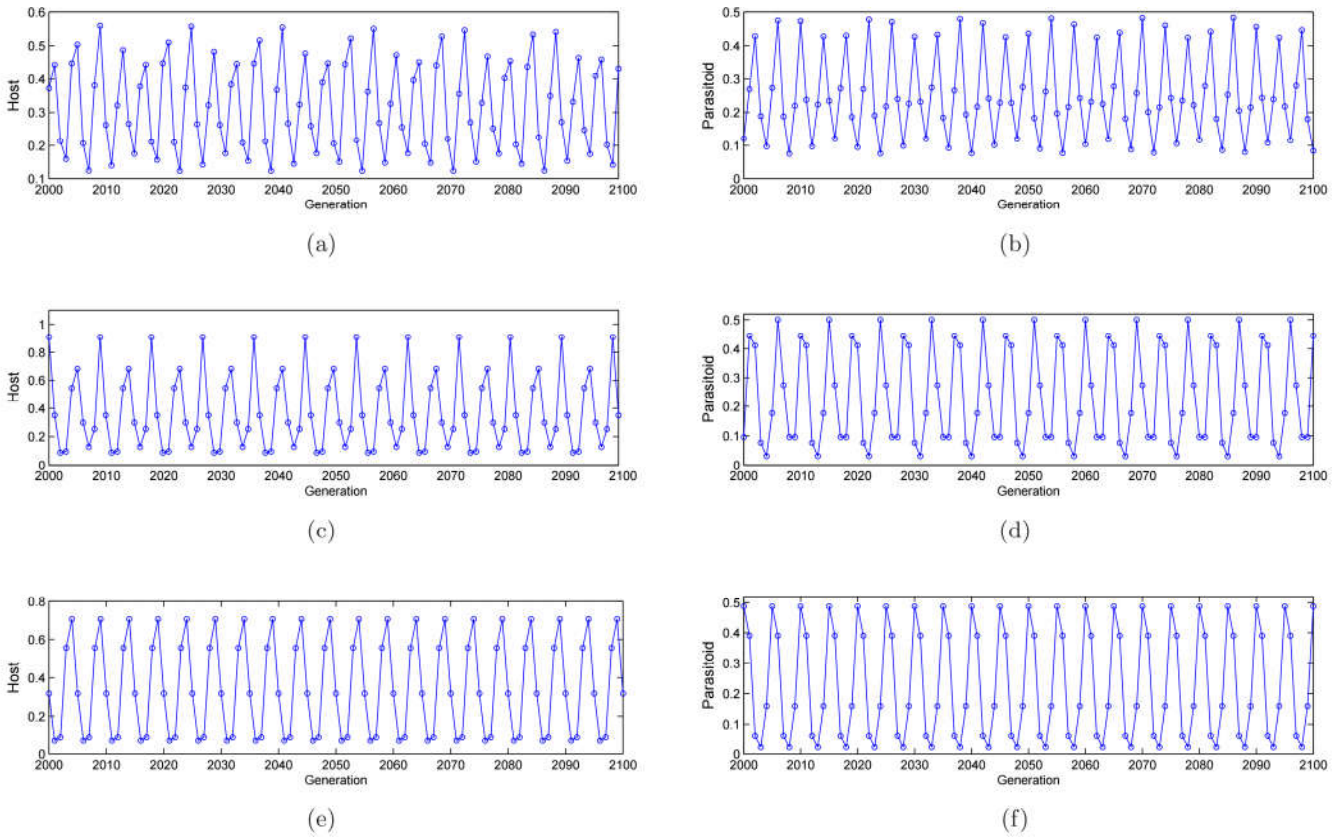

Fig. 9. Three coexisting attractors of system (7) with different initial values. The initial values from top to bottom are $(H_0, P_0) = (0.5, 1.6)$, $(1.8, 1.6)$, and $(0.8, 0.3)$ respectively. (a) and (b) Periodic attractor with period 16; (c) and (d) periodic attractor with period 9; (e) and (f) periodic attractor with period 5. The other parameters are fixed as $r = 2.35$, $p = 0.5$, $ET = 0.3$, $\beta = 5$, $\tau = 0.1$, $k = 1$.

that different host-parasitoid initial densities may result in different host-outbreak solutions. Another three host-outbreak attractors coexist as shown in Fig. 9. From pest control point of view, the integrated control strategies may strictly depend on the initial densities of both populations. Because different attractors have different outbreak amplitudes and different outbreak frequencies.

Figures 8 and 9 indicate that in order to control the host population successfully such that its density decreases and falls below ET, the initial densities of both host and parasitoid populations should be monitored and tracked carefully. The basins of attraction with respect to three different host-outbreak solutions of coexistence are shown in Fig. 10. The horizontal axis and vertical axis are the host and parasitoid initial values, respectively. In Fig. 10(a), the initial value ranges are $0 \le H_0 \le 3$, $0 \le P_0 \le 2$ and Fig. 10(b) is an enlargement of the Fig. 10(a) with range $0 \le H_0 \le 1$, $0 \le P_0 \le 1$. Figure 10 illustrates the basins of attraction for three host attractors — the purple, yellow and green areas are the attraction regions for the periodic solutions shown in Figs. 8(a)–8(c), respectively. According to the amplitudes of periodic attractors shown in Fig. 8, we conclude that the purple area may be an ideal initial area for host control. Other basins of attraction of two coexisting attractors are shown in Fig. 11. Note that the fractal properties of the basins of attraction self-similarity and fractal basin boundaries can be clearly seen from the two basins of attraction. Moreover, we can also see that the line $H_0 = ET$ separates the attraction regions into two parts, which reveal different patterns.

4.3. *Switch-like behavior*

To understand how the different number of natural enemies releases (here parasitoid) affect the final state of the host population, we rewrite the subsystem S_{G_2} as follows

$$S_{G_2}(t+1) = [(1-p)H(t)e^{r(1-\frac{H(t)}{K})-\beta P(t)}, \quad H(t)(1-e^{-\beta P(t)}) + \tau_t]^T \qquad (18)$$

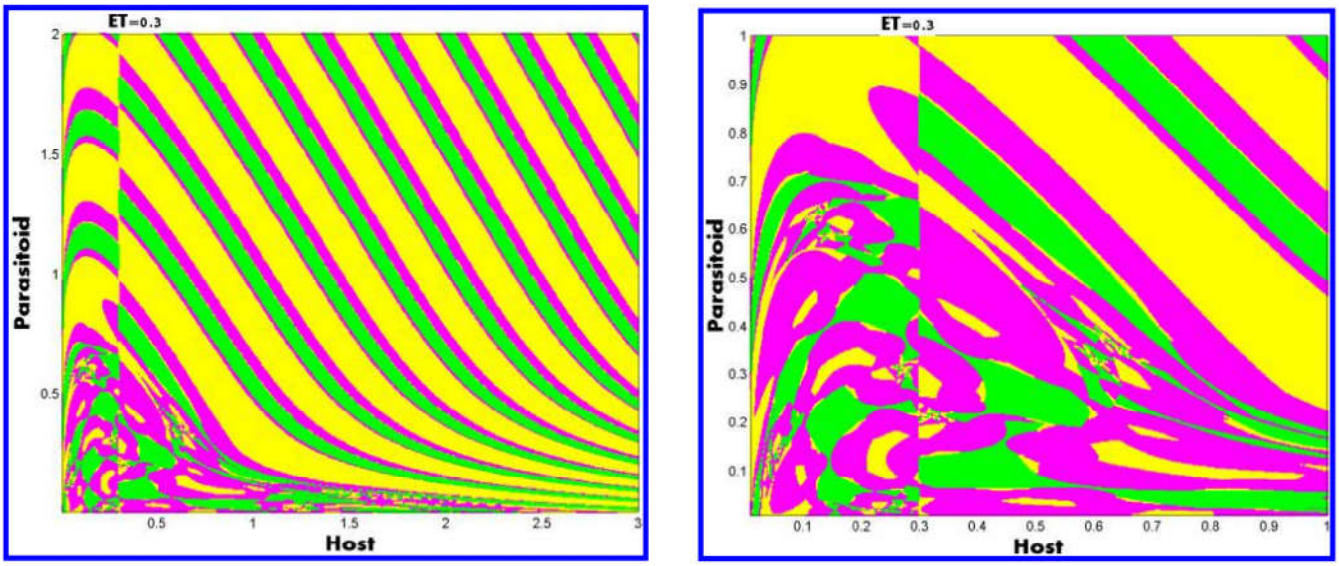

(a) (b)

Fig. 10. Basins of attraction of three coexisting attractors of system (7), the horizontal axis and vertical axis are the host and parasitoid initial value H_0, P_0 respectively. (a) Basin of attraction of three periodic solutions shown in Fig. 8, where the intervals of initial values are $0 \leq H_0 \leq 3$, $0 \leq P_0 \leq 2$ and (b) an enlargement of (a) with range $0 \leq H_0 \leq 1$, $0 \leq P_0 \leq 1$. The other parameters are fixed as $r = 2.35$, $p = 0.5$, $ET = 0.3$, $\beta = 5$, $\tau = 0.1$, $k = 1$.

where $\tau_t = \tau$ (without random perturbation at generation t) or $\tau_t = \tau + \sigma u$ (with random perturbation at generation t), u is a variable uniformly distributed on $[-1, 1]$ and $\sigma > 0$ represents the intensity of noise. What we want to address is how the intensity of noise affects the host-outbreak amplitudes and whether the stable attractors switch from one attractor to another or not.

To show this, we fix the initial values $(H_0, P_0) = (0.1, 0.5)$ and the other parameters as those in Fig. 12. If we randomly perturb the releasing constant τ every 100 generations with an intensity

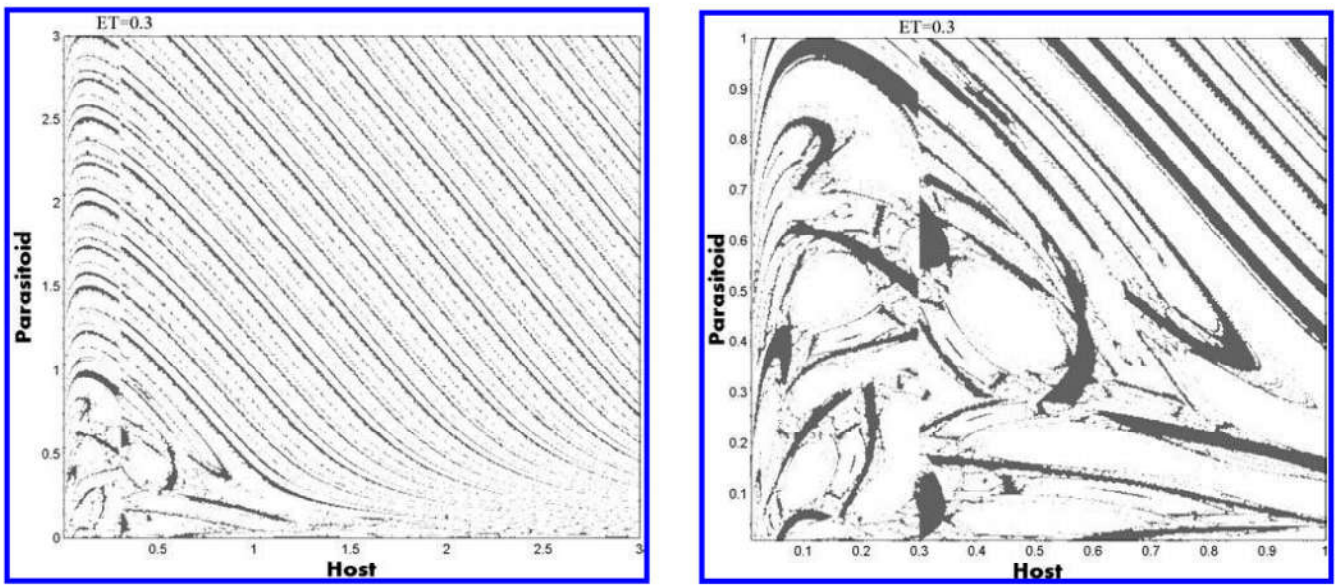

(a) (b)

Fig. 11. Basins of attraction of two attractors of system (7), the horizontal axis and vertical axis are the host and parasitoid initial value H_0, P_0 respectively. (a) Two periodic solutions coexist with $0 \leq H_0 \leq 3$, $0 \leq P_0 \leq 3$ and (b) an enlargement of (a) with range $0 \leq H_0 \leq 1$, $0 \leq P_0 \leq 1$. The other parameters are fixed as $r = 2.52$, $p = 0.3$, $ET = 0.3$, $\beta = 5$, $\tau = 0.1$, $k = 1$.

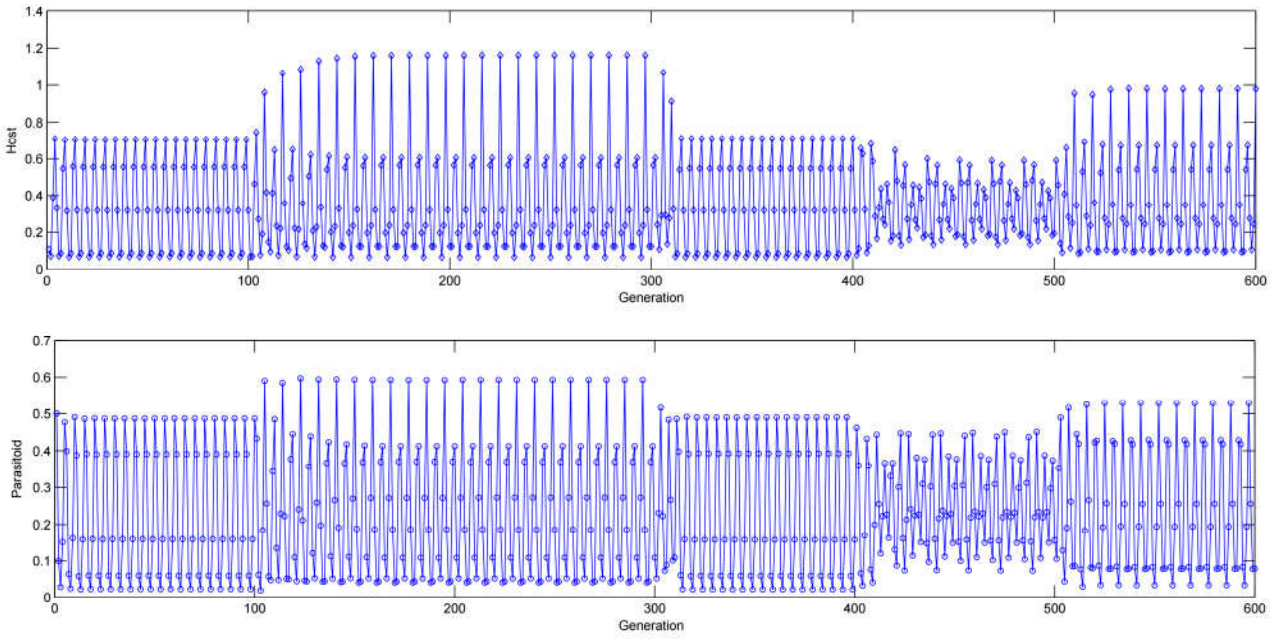

Fig. 12. Three attractors' switch-like behavior of system (4). Here the random perturbation has been applied at each, 100 generations. The other parameters are fixed as $r = 2.35$, $p = 0.5$, $ET = 0.3$, $\beta = 5$, $\tau = 0.1$, $k = 1$, $\sigma = 0.1$, the initial value $(H_0, P_0) = (0.1, 0.5)$.

$\sigma = 0.1$, then the attractors' switch-like behavior occurs. For example, within the first 100 generations the first stable attractor is the host-outbreak solution with medium amplitude. Once the random perturbation occurs at the 100th generation, the system quickly switches to the stable attractor with large amplitude. At the 200th generation the switching transient does not occur although the system experiences a random perturbation. Further, at the 300th generation, the second host-outbreak attractor can switch to the first attractor. At the 400th generation, the attractor can switch to third host-outbreak attractor with small amplitude again. Note that if we run the model continuously, then different switchings could occur among those three stable attractors, as those shown in Fig. 12.

To address the effects of different killing rates on the switched-like behavior, we rewrite the subsystem S_{G_2} as follows

$$S_{G_2}(t+1) = [(1-p_t)H(t)e^{r(1-\frac{H(t)}{K})-\beta P(t)}, \\ H(t)(1-e^{-\beta P(t)}) + \tau]^T \qquad (19)$$

where p_t is a random perturbation of p, which is defined as follows: $p_t = p$ (without random perturbation at generation t) or $p_t = p + \eta u$ (with random perturbation at generation t) and $\eta > 0$ represents the intensity of noise. By extensive numerical studies, we can see that the similar switched-like behavior can occur once the killing rate is randomly perturbed at every 100 generations with relatively large intensity (i.e. $\eta > 0.1$), as shown in Fig. 13.

4.4. *The key factors for switching frequencies*

In this section, we will discuss the effects of key parameters on the switching frequencies of system (7). For convenience, we provide the definition of switching frequencies as follows.

Definition 4.1. In system (7), if $H(t) \geq ET$ and $H(t+1) < ET$ (or $H(t) \leq ET$ and $H(t+1) > ET$), then we say the system experiences one time switch and t is called as switch-point. The interval between two switch-points is defined as switching frequency.

For successful pest control, the switching frequencies play an important role. For example, if the switchings occur frequently, then the control tactics must be applied more frequently, i.e. the pesticide applications and releasing strategies should be implemented frequently, and this is not cost effective and may result in adverse effects; if the patterns of switching frequencies are complex, then it is difficult to design suitable control measures for pest

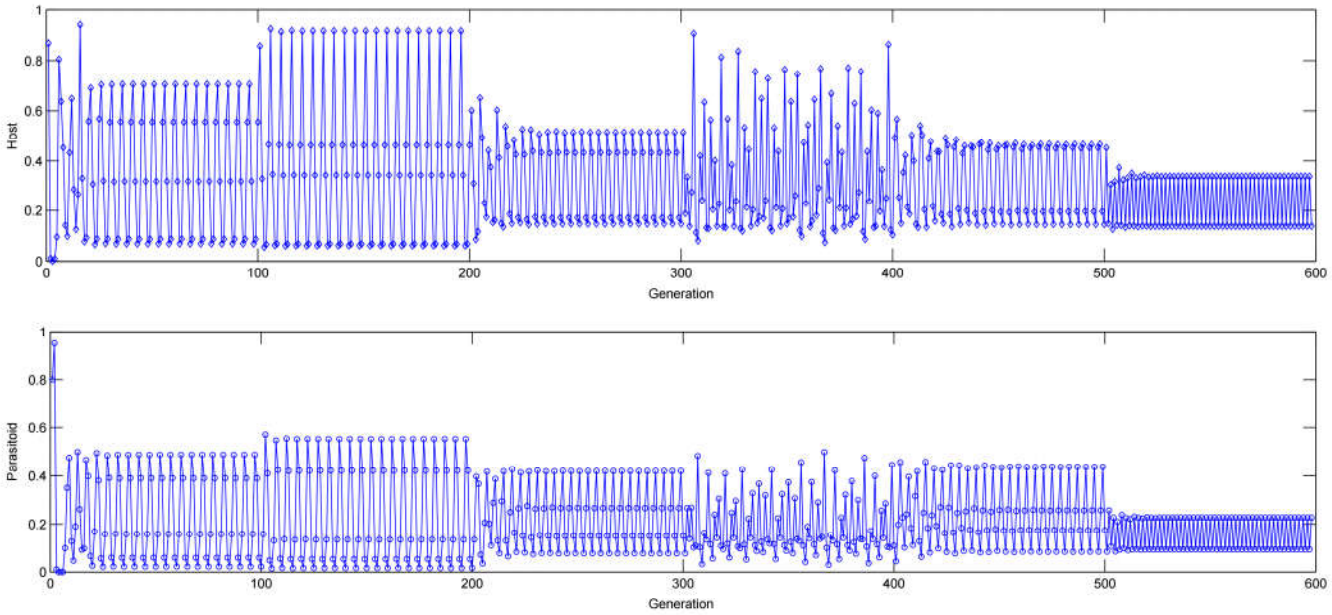

Fig. 13. Multiattractors' switch-like behavior of system (4). For each p plus a random disturbance for every 100 times. The other parameters are fixed as $r = 2.35$, $p = 0.5$, $ET = 0.3$, $\beta = 5$, $\tau = 0.1$, $k = 1$, $\eta = 0.1$, the initial value $(H_0, P_0) = (0.1, 0.5)$.

control since we do not know when and how control strategies should be adopted.

To address the effects of parameters on switching frequencies and number of switches, we let the initial values and intrinsic growth rates vary, as shown in Fig. 14, from which we can see that the switching frequencies have different patterns with different initial values and different intrinsic growth rates. For example, the switching frequencies with different initial values (here $(H_0, P_0) = (6, 3)$, (0.8, 0.5), (1.6, 0.8), respectively) are always unstable when $r = 3.3$, as shown in Figs. 14(a)–14(c), which can be confirmed by plotting the switching frequencies and number of switches, as shown in

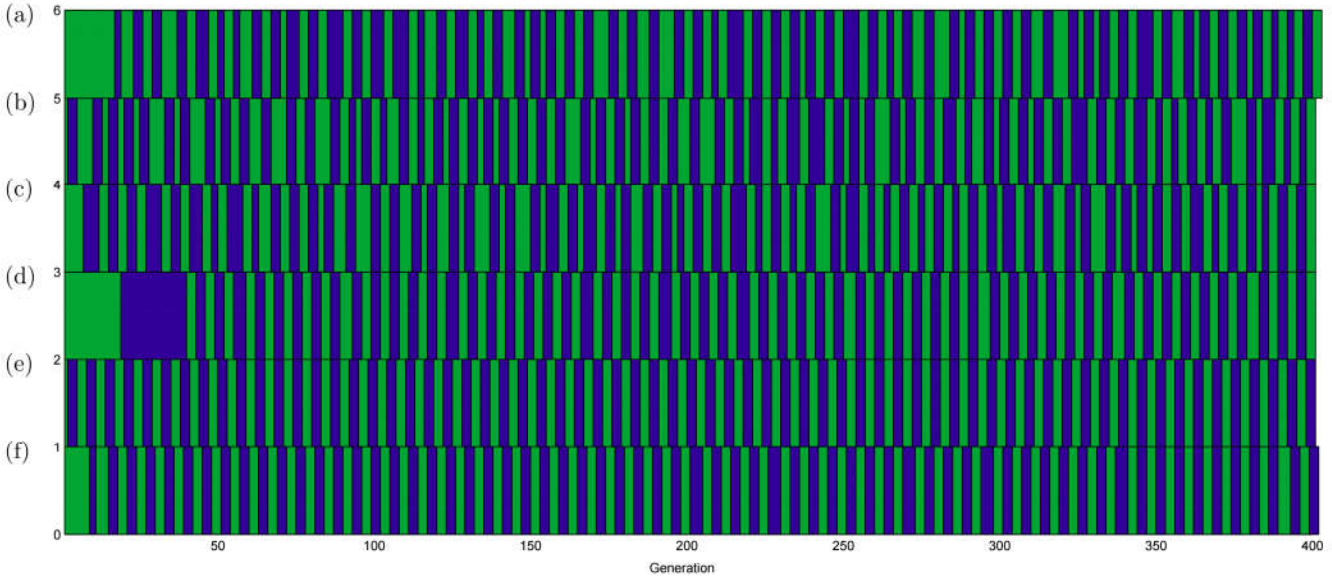

Fig. 14. Switching frequencies of system (4) about different r values and initial values with 400 generations. The green color regions denote the density of host population above ET (i.e. $H(t) \geq ET$) and the blue color regions denote the host density below ET (i.e. $H(t) < ET$). (a)–(c) $r = 3.3$ and initial values are $(H_0, P_0) = (6, 3)$, (0.8, 0.5), (1.6, 0.8) respectively and (d)–(f) $r = 2.7$ and initial values are $(H_0, P_0) = (6, 3)$, (0.8, 0.5), (1.6, 0.8), respectively. The other parameters are fixed as $ET = 0.5$, $\beta = 4$, $\tau = 0.1$, $k = 1$, $p = 0.5$.

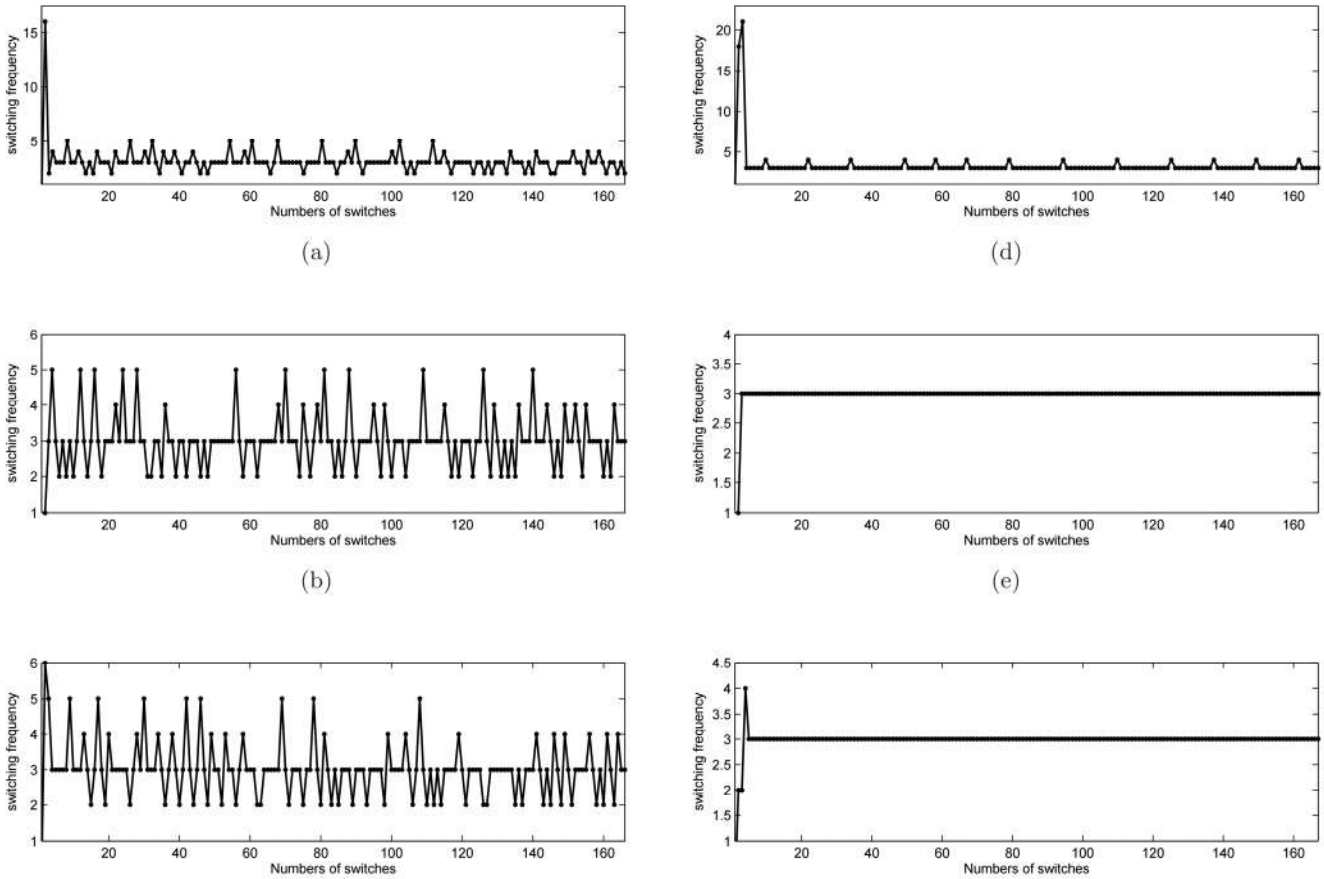

Fig. 15. Number of switches (166 time switches with 400 generations) and switching frequencies corresponding to Fig. 14.

Figs. 15(a)–15(c). However, if we fix the same initial values and $r = 2.7$, then the switching frequencies are eventually stable [see Figs. 14(d)–14(f), and Figs. 15(d)–15(f)] since the switching frequencies are stable at 3. Moreover, we find that the switching frequencies converge more quickly if the host-natural enemies ratio is relatively small. For example, the switching frequencies are stable when the system experiences period fluctuation switching for initial values $(H_0, P_0) = (6, 3)$ [see Fig. 15(d)]. Especially, the system just experiences two times or five times switching at $(H_0, P_0) = (0.8, 0.5)$ or $(H_0, P_0) = (1.6, 0.8)$ (see Fig. 15(e) or 15(f), respectively), and the switching frequencies quickly converge to three.

Similarly, we can investigate the effects of different killing rates on the switching frequencies. For example, the switching frequencies with different killing rates (i.e. $p = 0.1, 0.5, 0.8$) are eventually stable when $r = 2.7$, as shown in Figs. 16(a)–16(c). The results show that the smaller killing rates will lead to longer switching frequencies. Moreover, we find that there exists a long time vibration for large killing rate (i.e. $p = 0.9$) before the switching frequencies are stable, which is shown in Fig. 16(c). Furthermore, letting the released number τ vary, we observe that the switching frequencies display big variances, as shown in Figs. 17(a)–17(c). To compare Figs. 16 and 17, we can find that the chemical control is more effective than biological control to keep the switching frequencies remain stable.

In order to show more details of the effects of key parameters on switching frequencies, we first introduce the following definition

Definition 4.2. Mean switching frequency is the mean of all switching frequencies between 301 to 600 generation.

The effects of key parameters p, τ, ET and r on the mean switching frequency are shown in Fig. 18. It is shown that the mean switching frequency

Fig. 16. Switching frequencies with different p values. The parameters are fixed as $ET = 0.5$, $\beta = 4$, $\tau = 0.1$, $k = 1$, $r = 2.7$, and the initial values are fixed as $(H_0, P_0) = (0.8, 0.5)$. (a) $p = 0.1$, (b) $p = 0.5$ and (c) $p = 0.9$.

decreases as the intrinsic growth rate r increases, i.e. high intrinsic growth rates are associated with frequent switching. In Figs. 18(a) and 18(b), the mean switching frequency of the host population decreases for different ET (here $ET = 0.2$ and $ET = 0.5$). Most importantly, the mean switching frequency can suddenly jump from a small value to a larger value at some critical points of r, which implies that the selection of ET may be crucial in prolonging the pest outbreak period. Figures 18(c) and 18(d) indicate that the bigger killing rates (here $p = 0.2$ and 0.6) will lead to the smaller of mean switching frequency. Therefore, if we want to prolong the pest outbreak period, we should let the mean switching frequency be smaller. Figures 18(e) and 18(f) show that when r is bigger (here $r = 2.7$), the mean switching frequency decreases and is gradually stabilized. Moreover, when τ is bigger,

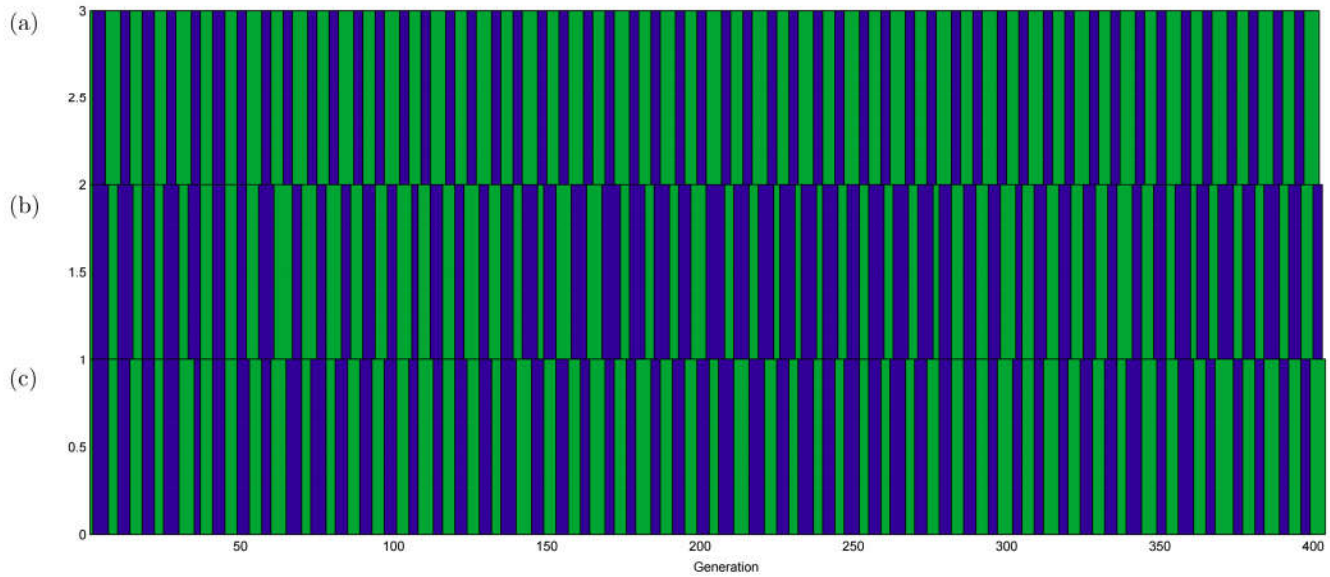

Fig. 17. Switching frequencies with different τ values. The parameters are fixed as $ET = 0.5$, $\beta = 4$, $p = 0.1$, $k = 1$, $r = 2.7$, and the initial values are fixed as $(H_0, P_0) = (0.8, 0.5)$. (a) $\tau = 0.1$, (b) $\tau = 0.2$ and (c) $\tau = 0.3$.

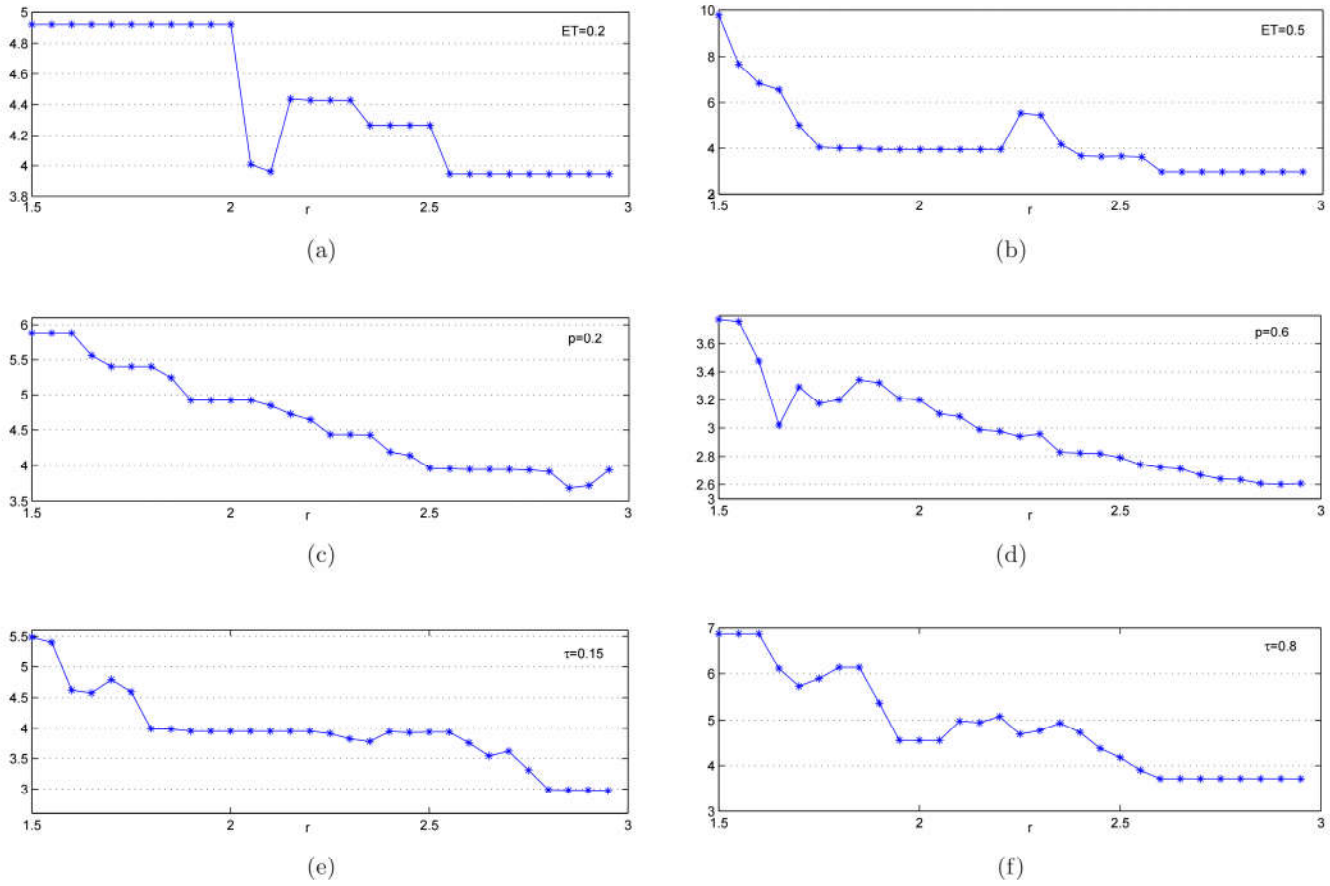

Fig. 18. Mean switching frequencies with r changing from $[1.5, 3]$. For each mean switching frequency, the first 300 generations are omitted to remove the initial transients and only the generations between 301 and 600 are plotted. (a) and (b) $\beta = 4$; $\tau = 0.1$, $k = 1$, $p = 0.5$; (c) and (d) $\beta = 4$, $\tau = 0.1$, $k = 1$, $ET = 0.5$; (e) and (f) $\beta = 4$, $\tau = 0.1$, $k = 1$, $ET = 0.5$, $p = 0.5$. The initial values are fixed as $(H_0, P_0) = (0.2, 0.5)$.

the mean switching frequency becomes longer. It implies that if we aim to prolong the pest outbreak period, we can release more natural enemies.

5. Discussion

As mentioned in the introduction, the ET is an important factor in IPM strategy. We need to keep track of host (pest) populations for an IPM and keep the pest density below ET. In this paper, we discussed the switching discrete host-parasitoid model with IPM which is extended from the classical Nicholson–Bailey model. In the switching model, control measures — switching strategies — are guided by the ET. This switching system is divided into two subsystems, the control-free subsystem S_{G_1} and controlled subsystem S_{G_2}.

We discussed the existence and stability of several types of equilibria of the full switching system. We gave two- or three-parameter bifurcation diagrams that reveal the regions of different types of equilibria including regular and virtual equilibria. We numerically showed the existence of different types of equilibria and the coexistence in parameters r–ET coordinate plane [see Fig. 2(a)]. We noted that if the parameters β and ET vary simultaneously, the equilibrium regions of S_{G_1} and S_{G_2} are changed from regular to virtual, or from virtual to regular [see Fig. 2(b)]. Thus, from the perspective of pest management, appropriate control strategies and ET can be designed such that the interior equilibrium of S_{G_1} is regular, and the interior equilibrium of S_{G_2} is virtual.

Our bifurcation diagram of parameter p indicated that the host population can stabilize in subsystem S_{G_1} (see Fig. 5). The interaction between host and parasitoid plays a very important role in pest control, and the control tactics should be designed to take into account this interaction. Morever, the initial densities of host and parasitoid populations affect the control strategies (see Fig. 6),

and our analysis showed five different possible cases (always be free, be free from one time, two times, three times, and several times IPM). Examining the host densities and the parasitoid densities plane (see Fig. 7),we observed that different host-parasitoid initial densities as well as host-parasitoid ratios may result in different final states of the host population.

The bifurcation diagram of parameter r provided evidence that the switching discrete system may have very complex dynamics including the coexistence of multiple attractors and switched-like behavior among attractors (see Fig. 3). To confirm the coexistence of multiple attractors and discuss their biological implications, we fixed all parameters as those in Fig. 8 and chose different initial densities to show that there exist three host-outbreak attractors at $r = 2.54$ and these host-outbreak attractors display different amplitudes and frequencies. Therefore, the IPMS may strictly depend on the initial densities of both populations. In order to control the host population successfully such that its density decreases and falls below ET, the initial densities of both host and parasitoid populations should be monitored and tracked carefully. The basins of attraction with respect to three different host-outbreak solution of coexistence are shown in Fig. 10, with the purple area being an ideal initial area for host control, the green area being an undesirable area for control because the pesticide applications and releasing strategies should be implemented frequently. To address the effects of the different number of natural enemies releases and different killing rates, we randomly perturbed the releasing constant τ or p every 100 generations, and we noted that attractors' switch-like behavior occurs (see Figs. 12 and 13).

Finally, we considered how the key parameters and initial values of both host and parasitoid populations affect the host outbreaks, switching frequencies or mean switching frequency, and consequently the relative biological implications with respect to pest control are discussed. For successful pest control, the switching frequencies play an important role. If the patterns of switching frequencies are complex, then it is difficult to design suitable control measures for pest control due to the unpredictable nature of when and how control strategies should be adopted [see Figs. 14(a)–14(c) and 15(a)–15(c)]. If the patterns of switching frequencies are stable, the switching frequencies converge more quickly if the host-natural enemies ratio is relatively small [see Figs. 14(d)–14(f) and 15(d)–15(f)]. In order to show the effects of key parameters p, τ, ET and r on switching frequencies, we generated Fig. 18 that shows that the mean switching frequency decreases as the intrinsic growth rate r increases, i.e. high intrinsic growth rates are associated with frequent switching.

In a real world, the host populations have different growth, and the parasitoid populations can affect host density at different ET. So, we should consider this switching discrete system with functional response and discuss the switching discrete system with Beverton–Holt growth. We leave these to a future investigation.

Acknowledgments

This work was partially supported by the National Natural Science Foundation of China (11171199, Sanyi Tang), and by the Fundamental Research Funds for the Central Universities (GK201305010, GK201401004, Sanyi Tang), and by Key Laboratory of Biologic Resource Protection and Utilization of Hubei Province (PKLHB1332, Changcheng Xiang), and by the Natural Science Foundation of Hubei Province (CDZ2010047, Changcheng Xiang), and the Soft Science Research project of Hubei Province (2012GDA01309, Zhongyi Xiang), and by the Natural Sciences and Engineering Research Council of Canada (Jianghong Wu).

References

Bischi, G.-I., Lamantia, F. & Radi, D. [2013] "A prey–predator fishery model with endogenous switching of harvesting strategy," *Appl. Math. Comput.* **219**, 10123–10142.

Bischi, G. I., Lamantia, F. & Tramontana, F. [2014] "Sliding and oscillations in fisheries with on–off harvesting and different switching times," *Commun. Nonlin. Sci. Numer. Simulat.* **19**, 216–229.

Blommers, L. H. [1994] "Integrated pest management in European apple orchards," *Ann. Rev. Entomol.* **39**, 213–241.

Cabello, T., Gallego, J. R., Fernandez, F. J., Gamez, M., Vila, E., Pino, M. D. & Hernandez-Suarez, E. [2012] "Biological control strategies for the South American tomato moth (lepidoptera: Gelechiidae) in greenhouse tomatoes," *J. Econ. Entomol.* **105**, 2085–2096.

Ceccato, P., Cressman, K., Giannini, A. & Trzaska, S. [2007] "The desert locust upsurge in West Africa (2003–2005): Information on the desert locust early warning system and the prospects for seasonal climate forecasting," *Int. J. Pest Manag.* **53**, 7–13.

da Silveira Costa, M. I. & Meza, M. E. M. [2006] "Application of a threshold policy in the management of multispecies fisheries and predator culling," *IMA Math. Med. Biol.* **23**, 63–75.

Dercole, F., Gragnani, A. & Rinaldi, S. [2007] "Bifurcation analysis of piecewise smooth ecological models," *Theor. Popul. Biol.* **72**, 197–213.

Elaydi, S. [2005] *An Introduction to Difference Equations*, Vol. 2 (Springer, NY).

Grainge, M. & Ahmed, S. [1988] *Handbook of Plants with Pest-Control Properties* (John Wiley, NY).

Hassell, M. P. & May, R. M. [1973] "Stability in insect host-parasite models," *J. Anim. Ecol.* **42**, 693–726.

Heinrichs, E. & Mochida, O. [1984] "From secondary to major pest status: The case of insecticide-induced rice brown planthopper, nilaparvata lugens, resurgence," *Prot. Ecol.* **7**, 201–218.

Helyer, N., Cattlin, N. D. & Brown, K. C. [2014] *Biological Control in Plant Protection*: *A Colour Handbook*, 2nd edition (CRC Press).

Higley, L. G. & Pedigo, L. P. [1996] *Economic Thresholds for Integrated Pest Management*, Vol. 9 (University of Nebraska Press).

Hoffmann, M. P. & Frodsham, A. [1993] *Natural Enemies of Vegetable Insect Pests* (A Cornell Coop. Ext. Publ., Cornell University).

Holt, J. & Cheke, R. A. [1996] "Models of desert locust phase changes," *Ecol. Model.* **91**, 131–137.

Jenser, G., Balázs, K., Erdélyi, C., Haltrich, A., Kádár, F., Kozár, F., Markó, V., Rácz, V. & Samu, F. [1999] "Changes in arthropod population composition in IPM apple orchards under continental climatic conditions in Hungary," *Agr. Ecosyst. Environ.* **73**, 141–154.

Liang, J. & Tang, S. [2010] "Optimal dosage and economic threshold of multiple pesticide applications for pest control," *Math. Comput. Model.* **51**, 487–503.

Liang, J., Tang, S., Cheke, R. A. & Wu, J. [2013] "Adaptive release of natural enemies in a pest-natural enemy system with pesticide resistance," *Bull. Math. Biol.* **75**, 2167–2195.

Mitchell, C. E. & Power, A. G. [2003] "Release of invasive plants from fungal and viral pathogens," *Nature* **421**, 625–627.

Moran, P. [1950] "Some remarks on animal population dynamics," *Biometrics* **6**, 250–258.

Mound, L. A. & Halsey, S. H. [1978] *Whitefly of the World. A Systematic Catalogue of the Aleyrodidae (Homoptera) with Host Plant and Natural Enemy Data* (John Wiley, NY).

Murray, J. D. [2002] *Mathematical Biology I*: *An Introduction*, 3rd edition (Springer, NY).

Parker, F. D. [1971] "Management of pest populations by manipulating densities of both hosts and parasites through periodic releases," *Biological Control* (Springer, US), pp. 365–376.

Reed, G. L., Jensen, A. S., Riebe, J., Head, G. & Duan, J. J. [2001] "Transgenic BT potato and conventional insecticides for colorado potato beetle management: Comparative efficacy and non-target impacts," *Entomol. Exp. Appl.* **100**, 89–100.

Ricker, W. E. [1954] "Stock and recruitment," *J. Fish. Res. Board Can.* **11**, 559–623.

Rohani, P. & Ruxton, G. D. [1999] "Dispersal-induced instabilities in host parasitoid metapopulations," *Theor. Popul. Biol.* **55**, 23–36.

Settle, W. H., Ariawan, H., Astuti, E. T., Cahyana, W., Hakim, A. L., Hindayana, D., Lestari, A. S. & Pajarningsih, S. [1996] "Managing tropical rice pests through conservation of generalist natural enemies and alternative prey," *Ecology* **77**, 1975–1988.

Smith, R. F., Apple, J. L. & Bottrell, D. G. [1976] "The origins of integrated pest management concepts for agricultural crops," *Integrated Pest Management* (Springer), pp. 1–16.

Tang, S., Xiao, Y. & Cheke, R. A. [2008] "Multiple attractors of host-parasitoid models with integrated pest management strategies: Eradication, persistence and outbreak," *Theor. Popul. Biol.* **73**, 181–197.

Tang, S., Liang, J., Xiao, Y. & Cheke, R. A. [2012] "Sliding bifurcations of Filippov two stage pest control models with economic thresholds," *SIAM J. Appl. Math.* **72**, 1061–1080.

Tang, S., Liang, J., Tan, Y. & Cheke, R. A. [2013] "Threshold conditions for integrated pest management models with pesticides that have residual effects," *J. Math. Biol.* **66**, 1–35.

Van Lenteren, J. & Woets, J. V. [1988] "Biological and integrated pest control in greenhouses," *Ann. Rev. Entomol.* **33**, 239–269.

Wolf, P. & Verreet, J. [2002] "An integrated pest management system in Germany for the control of fungal leaf diseases in sugar beet: The IPM sugar beet model," *Plant Dis.* **86**, 336–344.

Wright, M. G., Kuhar, T. P., Hoffmann, M. P. & Chenus, S. A. [2002] "Effect of inoculative releases of trichogramma ostriniae on populations of ostrinia nubilalis and damage to sweet corn and field corn," *Biol. Contr.* **23**, 149–155.

Xiao, Y., Xu, X. & Tang, S. [2012] "Sliding mode control of outbreaks of emerging infectious diseases," *Bull. Math. Biol.* **74**, 2403–2422.

Xiao, Y., Miao, H., Tang, S. & Wu, H. [2013] "Modeling antiretroviral drug responses for HIV-1 infected patients using differential equation models," *Adv. Drug Deliv. Rev.* **65**, 940–953.

Zhao, T. & Xiao, Y. [2013] "Non-smooth plant disease models with economic thresholds," *Math. Biosci.* **241**, 34–48.